Local Atomic Structures at Grain Boundaries in Gadolinium Doped Cerium Oxides

Tomomi Kosaka[1*], Kiminori Sato[2]

[1]*Department of Chemistry, Tokyo Gakugei University, Tokyo, Japan,*
[2]*Department of Environmental Science, Tokyo Gakugei University, Tokyo, Japan*

(Received February 28, 2010 ; Final form May 12, 2010)

ABSTRACT

Gadolinium doped ceria (GDC) prepared by coprecipitation method was investigated by x-ray diffraction (XRD), complex impedance measurement, and positron lifetime spectroscopy. The grain boundary conductivity was found to be lower than that of bulk conductivity. XRD revealed the fluorite structure indicating that gadolinium is successfully doped into cerium oxide. Prior to sintering, the vacancy-sized free volume and nanovoid were observed at interfaces among crystallites. The vacancy-sized free volumes shrank with increasing sintering temperatures and finally got dominant. The results suggest that the sintering process of GDC follows the kinetics of vacancy-sized free volumes and nanovoids at interfaces.

Keywords: GDC, solid state electrolyte, sintering, positron lifetime spectroscopy

*E-mail: tkosaka@u-gakugei.ac.jp

1. INTRODUCTION

Gadolinium doped ceria (GDC) is one of the promising candidate for electrolyte /1-6/ of solid oxide fuel cell owing to high conductivity of oxygen ions in the intermediate temperature range (773-973K). Substitution from Ce^{4+} to Gd^{3+} produces oxygen vacancies for compensating electric charge. Since the ionic radius of Gd^{3+} is similar to that of Ce^{4+}, gross distortion isn't expected in ceria host lattice. The excess oxygen vacancies lead to higher ionic conductivity than for undoped ceria.

It has been suggested that oxygen ionic conductivity of ceria based electrolyte is influenced by constituent grains. Sameshima et al. /7/ reported that the grain resistance for the diffusion of oxygen ions is responsible for ionic conductivity for rare-earth doped ceria prepared by coprecipitation method. In principle, high temperature sintering over at 1573K is required for GDC to achieve density more than 90% with less open porosity. Such high temperature causes a replacement from CeO_2 to Ce_2O_3, which leads to produce micro-cracks along with the degradation of conduction efficiency. Takamura et al. /8/ observed an enhancement of electric conductivity under the pressure of Gigapascal

for acceptor-doped ceria nanoparticles. They attributed the enhancement of electric conductivity under high pressure to the densification of granular particles.

Positrons preferentially localize at atomic disorder as e.g., grain boundary /9/, and provide us the information on local atomic structures at annihilation sites /10-11/. Some experiments by positron annihilation spectroscopy predicted the presence of vacancy-like defects and larger free volumes associated with interfaces among crystallites for zirconia-based materials /12-13/. Garay et al./13/ proposed that defects in negatively charged grain-boundary space region correspond to positron trapping sites, since positrons are not trapped by positively charged spaces such as oxygen vacancies.

Here, our advances in the study of GDC by XRD, complex impedance measurement, and positron lifetime spectroscopy are described/14/. We focus on the evolution of local atomic structures at interfaces upon sintering to gain an insight into the densification mechanism.

2. EXPERIMENTAL PROCEDURE

2.1. Materials

GDC was prepared by oxalate coprecipiation method /15/. The starting materials were $Ce(NO_3)_3{\cdot}6H_2O$, $Gd(NO_3)_3{\cdot}6H_2O$, $H_2C_2O_4{\bullet}2H_2O$. All reagents were purchased from Wako Pure Chemical industries LTD. The cerium and gadolinium nitrate solutions (0.2mol/l) were mixed at a molar ratio of gadolinium of approximately 0.2. The mixed solution was dropped into a stirred oxalic acid solution (0.4mol/l) to produce oxalate coprecipitate. The coprecipitate was filtered, washed with ion exchanged water in several times, and dried at 313K for 8h. The oxalate coprecipitate was calcined at 873K in air for 1h to form GDC. The GDC powders were uniaxially pressed into a pellet with 10mm diameter and 2mm thickness under the pressure of 20MPa. The GDC pellets were sintered from 873K to 1273K for 6h in air.

2.2. Characterization

The lattice parameters of GDC were calculated from diffracted peaks measured by Cu Kα X-ray diffractmeter (Ultima IV, Rigaku corp.) operated at 40kV, 50mA. The scattering angles were calibrated using Si powder (NIST 640c). The crystallite size of GDC was estimated from (111) diffraction peak by Scherrer's equation. The bulk density was measured by the Archimedes method using ion exchanged water. The Pt electrodes were formed on the both side of GDC pellet by heating at 1473 K using Pt paste (Tanaka Kikinzoku TR-7070). The oxygen ionic conductivity of the pellet was measured in air from 673K to 973K conducted by complex impedance analyzer (Princeton applied research corp. VersaSTAT3) in the frequency range from 100 μHz to 1MHz. The impedance data of GDC was analyzed using ZView software (Scribner Associates).

Positron lifetime spectroscopy was performed at room temperature. The positron source (^{22}Na), sealed in a thin foil of Kapton, was mounted in a sample-source-sample sandwich. Positron lifetime spectra (~ 10^6 coincidence counts) were recorded with a time resolution of 230 ps full-width at half-maximum (FWHM). The data were numerically analyzed using the POSITRONFIT code /16/.

3. RESULTS AND DISCUSSION

Figure 1 shows the XRD pattern of GDC sintered at 1073K for 6h in air. The XRD pattern indicates that GDC has a fluorite type structure without any other phases. The peaks denoted as Pt indicate the diffraction from sample holder. All peaks of GDC are shifted to low angle region against to the corresponded ones of CeO_2 (denoted as solid bar) indicating the expansion of interplanar spacing for GDC by Gd doping. The lattice parameter calculated for GDC is 0.54245 ±0.00006nm. Hong and Virkar /17/ reported that the lattice parameter, a for GDC is given by following equation:

$$a = \frac{4}{\sqrt{3}}[xr_1 + (1-x)r_2 + (1-0.25x)r_3 + 0.25xr_4] \times 0.9971$$

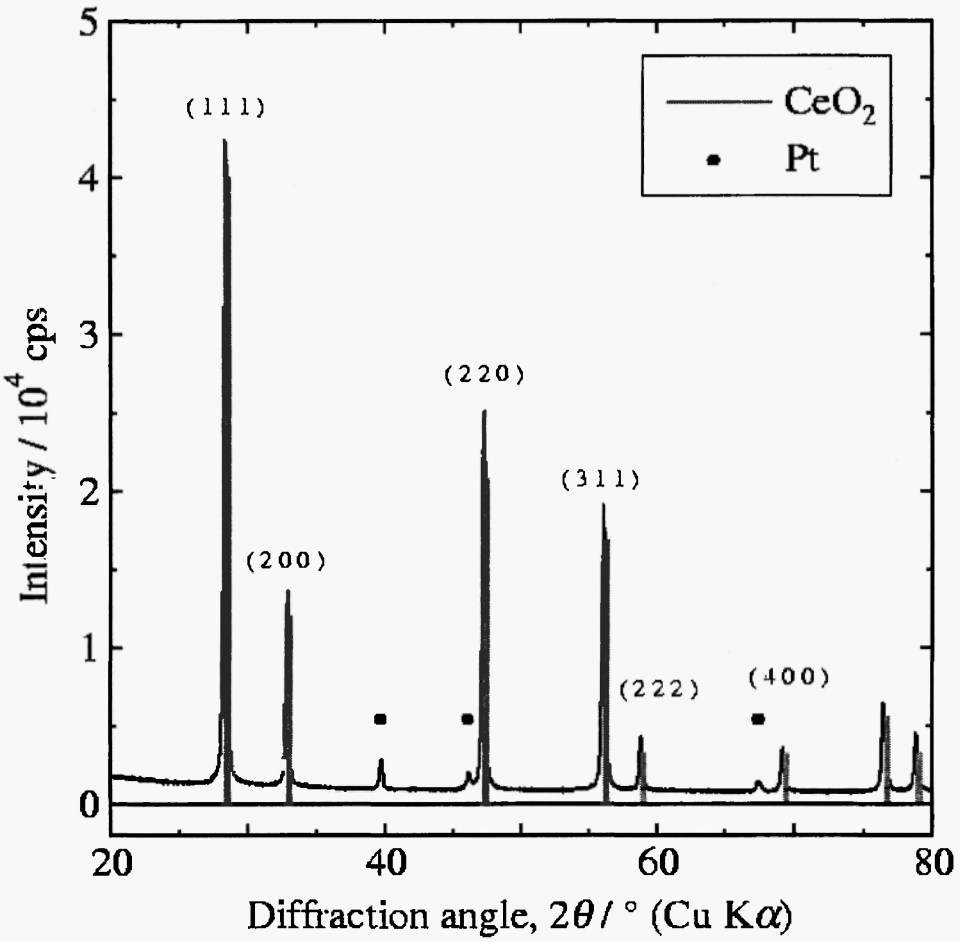

Fig. 1: XRD pattern of GDC sintered at 1073K for 6h in air. For comparison, the data of CeO_2 taken from JCPDS No.34-394 is added.

where x, r_1, r_2, r_3, and r_4 are the concentration of gadolinium ion, the radii of the gadolinium ion (0.1053nm), cerium ion (0.097nm), oxygen ion (0.138nm) and the oxygen vacancy (0.1164nm), respectively. The factor, 0.9971, was introduced for correcting the discrepancy between the lattice parameter measured for pure ceria (0.5411nm; JCPDS No.34-394) and the calculated value using this equation when $x = 0$. Using the calculated lattice parameter and this equation, the Gd composition in GDC is estimated to be 0.1969. Additional EDS measurements however revealed the Gd composition of □0.26, which is significantly higher than above estimation. Further exploration is required on this matter.

If the relative density of GDC is close to theoretical one, we can determine whether oxygen vacancy is formed or not/17/. In the case of our GDC sintered at 1273K, the relative density is 80%. It may be thus unsuitable to directly discuss the structure of GDC with the results of Archimedes method. Based on the results of XRD reported above and experimental evidence confirming the oxygen vacancy model/18/, we believe that substitution of Ce^{4+} with Gd^{3+} partially occurs and oxygen vacancies are successfully formed.

The typical complex impedance of samples consists of two semicircles in the Nyquist plot (**Figure 2(a)**). The impedance arc is interpreted with equivalent electrical circuits (**Figure 2(b)**). One semicircle in high frequency

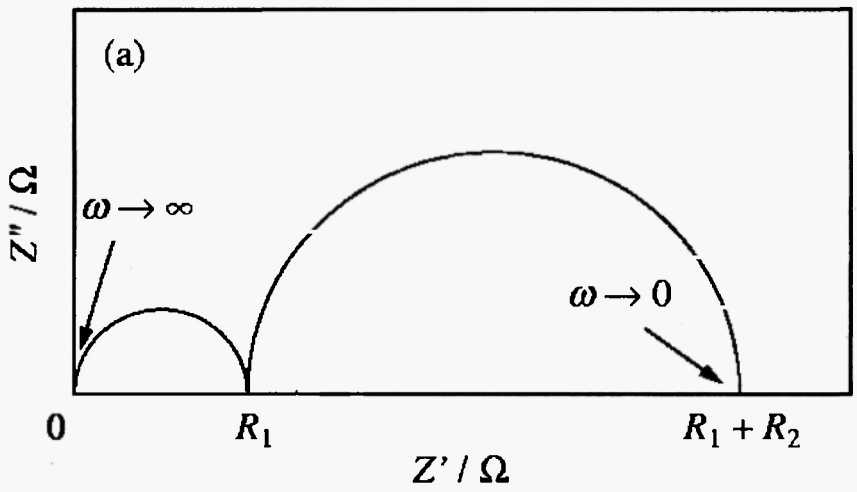

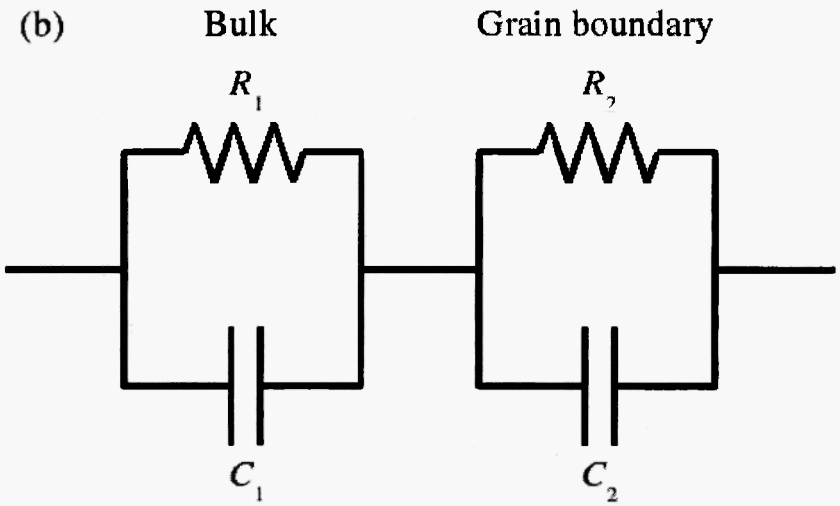

Fig. 2: Illustrations of (a) the Nyquist plot of typical complex impedance for GDC, (b) the equivalent electrical circuit for interpreting complex impedance of GDC.

range and the other in low frequency range may correspond to the oxygen migration in the bulk and across the grain boundaries, respectively. **Figure 3** shows the Arrhenius plots of the ionic conductivity calculated from bulk and grain boundary resistance for GDC and CeO_2. The conductivity of grain boundary is lower than that of bulk in both samples. The bulk conductivity of GDC at 773K is estimated to be 4.0×10^{-3} S cm^{-1}, which is 160 times higher than that of CeO_2. The bulk activation energy of 78.9 kJ /mol is obtained. This value is close to the result (75 kJ /mol) reported by Faber et al /19/. The activation energies of grain boundary for GDC and CeO_2 are relatively higher than that of bulk, suggesting that the diffusion of oxygen ion is affected by the local structural disorders at grain boundaries.

Figure 4 shows the results of positron lifetime spectroscopy for GDC. Prior to sintering, two components τ_1 (~ 260 ps) and τ_2 (~ 500 ps) corresponding to a vacancy-sized free volume and a

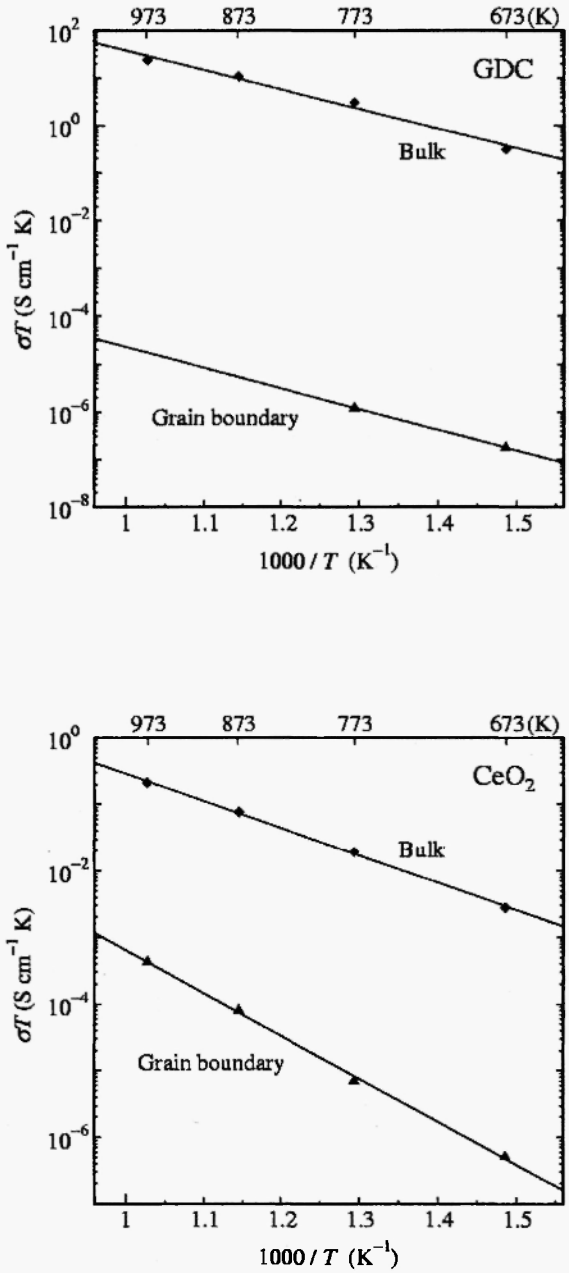

Fig. 3: Arrhenius plots of the ionic conductivity calculated from bulk and grain boundary resistance for GDC and CeO_2.

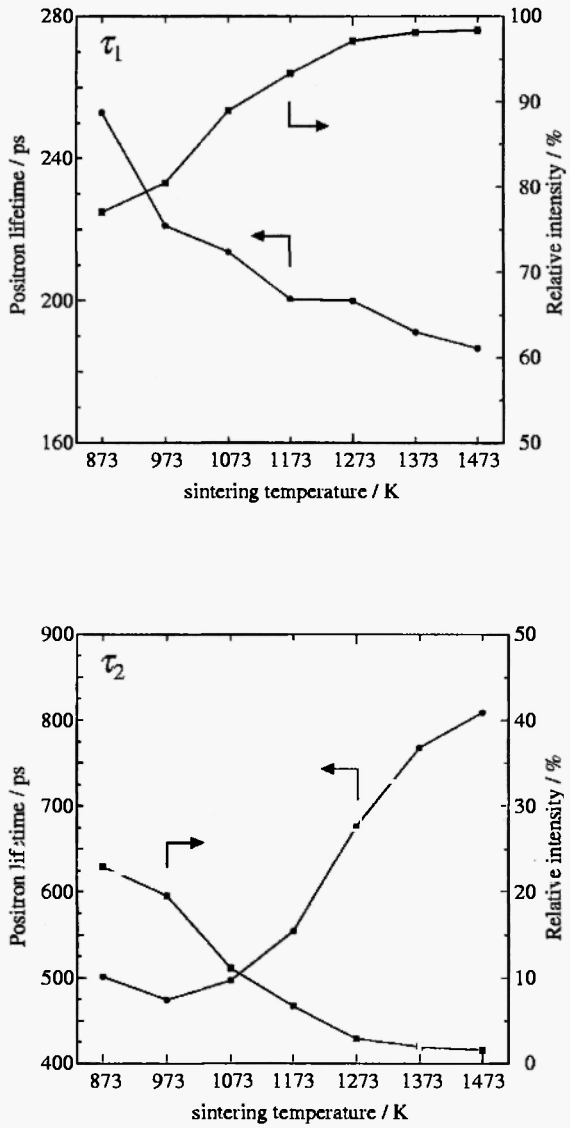

Fig. 4: Positron lifetimes (τ_1 and τ_2) and their relative intensities (I_1 and I_2) as a function of sintering temperatures.

nanovoid were obtained with their relative intensities I_1 (~ 80 %) and I_2 (~ 20 %), respectively. The average size of GDC crystallite evaluated from 311 peak broadening using Scherrer's equation is 12.8 nm before sintering, which is by far smaller than the typical positron diffusion length in solids of ~ 300 nm /20/. Positrons implanted in GDC crystallite can thus efficiently diffuse out and annihilate at interfaces among crystallites. We therefore conclude that the vacancy-sized free volumes and nanovoids are present at interfaces among crystallites. Similar observation was reported for yttria-stabilized zirconia by Čížek et al /12/.

With increasing temperatures the positron lifetime τ_1 decreases and its relative intensity I_1 increased, signifying shrinkage of vacancy-sized free volumes together with sintering. The lifetime τ_2 and its relative intensity I_2 exhibit the opposite tendency to those of vacancy-sized free volume. The vacancy-sized free volumes got dominant at the sintering temperature of 1473 K, while the nanovoids almost disappear. The results suggest that a substantial increase of local electron density at interfaces among crystallites occurs

as a result of sintering and the sintering process of GDC follows the kinetics of vacancy-sized free volumes and nanovoids at interfaces among crystallites.

4. CONCLUSION

We prepared gadolinium doped cerium oxide by oxalate coprecipitation method. XRD revealed that GDC has the fluorite structure with oxygen vacancies, indicating that gadolinium is successfully doped into cerium oxide. The bulk ionic conductivity of GDC sintered at 773K for 6h in air is 4.0×10^{-3} S / cm, which is 160 times higher than that of CeO_2. This result indicated that the oxygen vacancies have an influence on the bulk ionic conductivity effectively. Positron lifetime spectroscopy revealed the presence of vacancy-sized free volumes and nanovoids, of which the kinetics is associated with sintering.

ACKNOWLEDGEMENTS

This work was partially supported by Grants-in-Aid for Scientific Research from the Ministry of Education, Science, Sports and Culture of Japan (Grant Nos. 20740173 and 2154317). The authors would like to thank to Dr. K. Shinozaki (Tokyo Institute of Technology) for experimental assistance in the AC impedance measurement.

REFERENCES

1. H.Yahiro, T.Ohuchi, K.Eguchi and H.Arai, *J. Mater.Sci.*, **23**, 1036-1041(1988).
2. D. L. Maricle, T. E. Swarr and S. Karavolis, *Solid State Ionics*, **52**, 173-182(1992).
3. H.Inaba and H.Tagawa, *Solid State Ionics*, **83**, 1-16(1996).
4. M. Godickemeier, K.Sasaki, L.J. Gauckler, and I. Reiss. *J. Electrochem.Soc.*, **144** (5), 1635 (1997).
5. K.R.Reddy and K.Karan, *J. Electroceram.*, **15**, 45-56(2005).
6. L.D.Jadhav, M.G.Chourashiya, K.M.Subhedar, A.K.Tyagi and J.Y.Patil, *J. Alloys and Compounds*, **470**, 383-386(2009).
7. S.Sameshima, H.Ono, K.Higashi, K.Sonoda, Y.Hirata and Y.Ikuma, *J. Ceram. Soc. Japan*, **108**, 1060-1066 (2000).
8. H.Takamura, J.Kobayashi, N.Takahashi and M.Okada, *J. Electroceram.*, **22**, No.1-3, 24-32 (2009).
9. K. Sato, H. Murakami, W. Sprengel, H.-E. Schaefer, Y. Kobayashi, *Appl. Phys. Lett.* **94**, 1719041-1719043 (2009).
10. K. Sato, F. Baier, W. Sprengel, R. Würschum, and H.-E. Schaefer, *Phys. Rev. Lett.*, **92**, 127403 (2004).
11. K. Sato, D. Shanai, Y. Hotani, T. Ougizawa, K. Ito, K. Hirata, and Y. Kobayashi, *Phys. Rev. Lett.*, 96, 228302 (2006).
12. J.Čížek, O.Melikhova, J.kuriplach, I.Procházka, T.E.Konstantinova and I.A.Danilenko, *Phys. Stat. Sol. (c)*, **4**, 3847-3850 (2007).
13. J.E.Garay, S.C.Glade, P.Asoka-Kumer, U.Anselmi-Tamburini and Z.A.Munir, *J. Appl. Phys.*, 99, 024313(2006).
14. S. Ohta, T. Kosaka, and K. Sato, *Journal of Physics: Conference Series*, to be published.
15. S.Sameshima, H.Ono, K.Higashi, K.Sonoda and Y.Hirata, *J. Ceram. Soc. Japan*, **108**, 985-988(2000).
16. P.Kirkegaard and M.Eldrup, *Comput. Phys. Commun.*,**7**, 401-409 (1974).
17. S.J.Hong and A.V.Virkar, *J.Am.Ceram.Soc.*,**78**, No.2,433-439(1995).
18. T.H.Esell and S.N.Flengas, *Chem.Rev.*, **70**, 339-376(1970).
19. J.Faber, C.Geoffroy, A.Roux, A.Sylvestre and P.Abélard, *Appl.Phys.A*, **49**, 225-232(1989).
20. T. E. M. Staab, R. Krause-Rehberg and B. Kieback, *J. Mater. Sci.*, **34**, 3833-3851(1999).